

The topology of the C-terminal sections of the NCX1 Na⁺/Ca²⁺ exchanger and the NCKX2 Na⁺/Ca²⁺-K⁺ exchanger

Robert T. Szerencsei, Tashi G. Kinjo and Paul P.M. Schnetkamp*

Department of Physiology and Pharmacology; Hotchkiss Brain Institute; Faculty of Medicine; University of Calgary; Calgary, AB Canada

Keywords: Na/Ca exchanger, NCX, Na/Ca-K exchanger, NCKX, SLC8, SLC24, calcium homeostasis, membrane proteins

Abbreviations: SDS-PAGE, sodium dodecyl sulfate polyacrylamide gel electrophoresis; DTT, dithiothreitol; MALPEG, methoxy-polyethyleneglycol maleimide; FACS, fluorescence activated cell sorting; PBS, phosphate-buffered saline; EDTA, ethylenediaminetetraacetic acid; FCCP, carbonyl cyanide p-trifluoromethoxyphenylhydrazone; TBS, Tris-buffered saline; Tris, Tris(hydroxymethyl)aminomethane; PNGase, Peptide N-Glycosidase F; TMS, transmembrane segment; RIPA, radioimmunoprecipitation assay buffer; TBST, tris-base saline solution with tween

Mammalian Na⁺/Ca²⁺ (NCX) and Na⁺/Ca²⁺-K⁺ exchangers (NCKX) are polytopic membrane proteins that play critical roles in calcium homeostasis in many cells. Although hydrophathy plots for NCX and NCKX are very similar, reported topological models for NCX1 and NCKX2 differ in the orientation of the three C-terminal transmembrane segments (TMS). NCX1 is thought to have 9 TMS and a re-entrant loop, whereas NCKX2 is thought to have 10 TMS. The current topological model of NCKX2 is very similar to the 10 membrane spanning helices seen in the recently reported crystal structure of NCX_MJ, a distantly related archaeobacterial Na⁺/Ca²⁺ exchanger. Here we reinvestigate the orientation of the three C-terminal TMS of NCX1 and NCKX2 using mass-tagging experiments of substituted cysteine residues. Our results suggest that NCX1, NCKX2 and NCX_MJ all share the same 10 TMS topology.

Introduction

Members of the *SLC8* and *SLC24* gene families encode Na⁺/Ca²⁺ (NCX) and Na⁺/Ca²⁺-K⁺ exchangers (NCKX), respectively. NCX and NCKX are proteins found in the plasma membrane of most excitable cells and are responsible for Ca²⁺ extrusion after a rise of intracellular Ca²⁺ caused by prior activation of Ca²⁺ permeable channels. For example, NCX proteins play important roles in the heart, kidney and brain, while NCKX proteins play important roles in photoreceptors, olfactory neurons, brain and epidermal melanocytes.^{1–3} Hydrophathy analysis of all mammalian NCX and NCKX sequences reveals the presence of 12 hydrophobic segments, each long enough to form a transmembrane segment (TMS). The first putative TMS is at the N-terminus and thought to be a (partially) cleaved signal peptide.^{4,5} The remaining hydrophobic segments are organized in two clusters separated by a large hydrophilic loop and one of the hydrophobic segments is now thought to be part of this large hydrophilic loop and not a TMS. Current topological models suggest that the remaining hydrophobic segments form 9 TMS in NCX1^{6,7} and 10 TMS in NCKX2,^{8,9} the difference being a re-entrant loop thought to be present between TMS 7 and TMS 8 of NCX1 but not in NCKX2 (see Fig. 1). This means that the C-terminal

two TMS of NCX1 and NCKX2 have opposite orientations; this would place the C-terminus of NCX1 in the intracellular space while the C-terminus of NCKX2 faces the extracellular space. Recently, a high resolution crystal structure of a distantly related archaeobacterial Na⁺/Ca²⁺ exchanger (NCX_Mj) was obtained which lacks the signal peptide at the N-terminus but otherwise consists of 10 α -helical TMS¹⁰ in the same topological orientation previously reported for NCKX2. It should be pointed out that any sequence similarity is largely confined to TMS 2, 3, 7 and 8 which make up the so-called α repeats (Fig. 1) and are thought to be important for cation transport as they contain the cation binding sites in the NCX_MJ crystal structure¹⁰ and contain many residues substitution of which greatly affects cation transport in NCX1^{11,12} and NCKX2.^{13–16} In contrast, the TMS 4, 5, 9 and 10 show very little if any sequence similarity between the prokaryotic and mammalian exchangers or as for that matter between NCX1 and NCKX2. In order to reinvestigate the orientation of the C-terminal two TMS, we performed mass-tagging experiments in which we probe the accessibility of substituted cysteine residues in the C-terminal two TMS of both NCX1 and NCKX2 to the large hydrophilic sulfhydryl reagent polyethyleneglycol maleimide (MALPEG).¹⁷ Our results show the same orientation of the C-terminal two TMS in both NCX1 and NCKX2.

*Correspondence to: Paul P.M. Schnetkamp; Email: pschnetk@ucalgary.ca
Submitted: 01/30/13; Revised: 02/05/13; Accepted: 02/05/13
<http://dx.doi.org/10.4161/chan.23898>

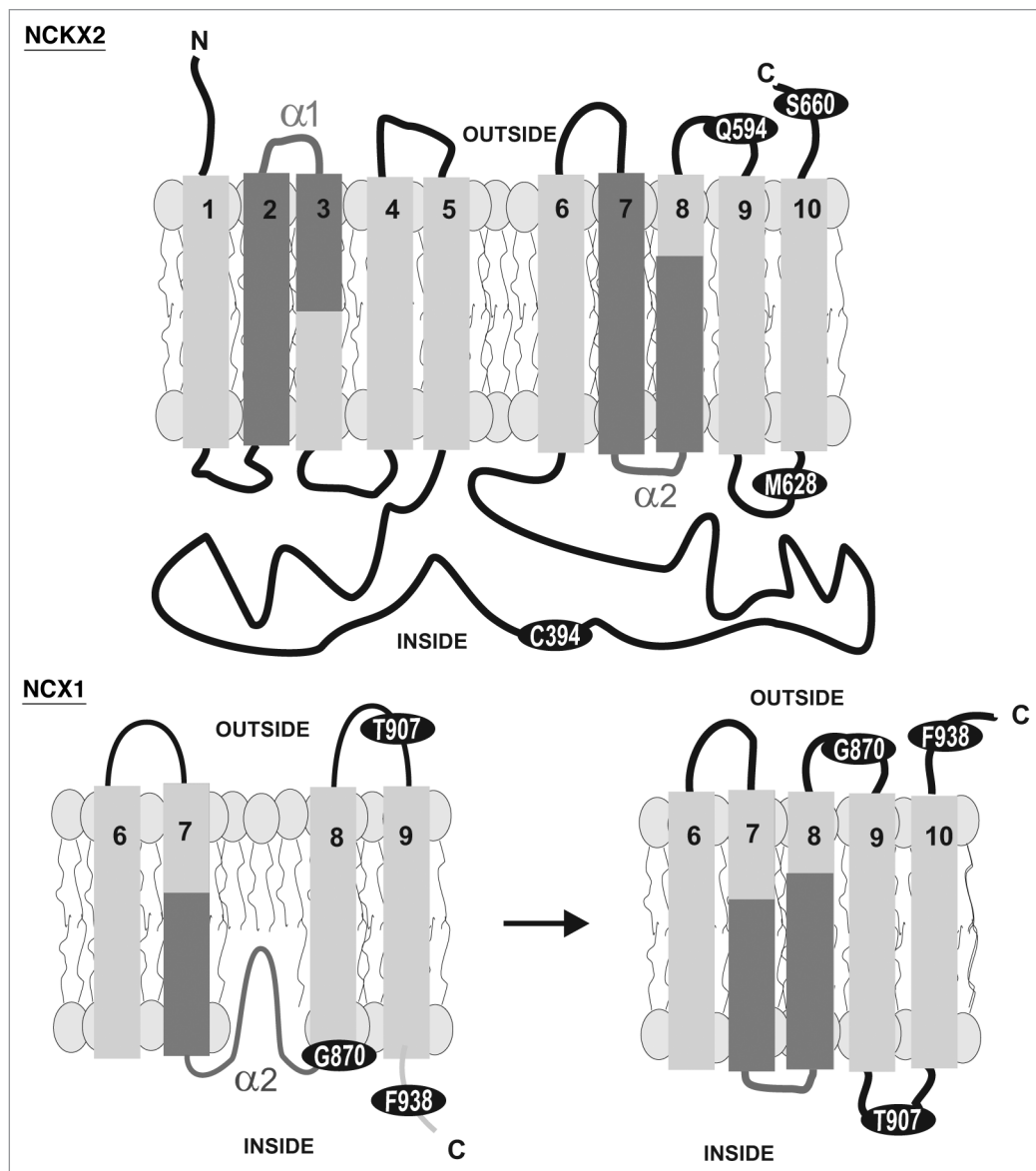


Figure 1. Topological models of NCKX2 and NCX1. The current topological model of NCKX2 is illustrated in the top panel; the two different C-terminal topological arrangements of NCX1 discussed in text are illustrated in the bottom panel. The dark gray bars indicate the location of the $\alpha 1$ and $\alpha 2$ repeats which are thought to have arisen from an ancient gene duplication event.²² The α repeats are the most conserved parts when comparing NCX or NCKX sequences from different isoforms or different species. The α repeats are also the only sequence elements that show any sequence similarity between NCX and NCKX.

This places the C-terminus facing the extracellular space which is consistent with the 10 TMS topology previously reported for NCKX2 and seen in the crystal structure of NCX_Mj.

Results

The cysteine-free dog NCX1 and human NCKX2 have previously been shown to express in cell lines and produce functional $\text{Na}^+/\text{Ca}^{2+}$ and $\text{Na}^+/\text{Ca}^{2+}/\text{K}^+$ exchangers, respectively.^{6,18} Since the published topological models for NCX1 and NCKX2 differ in the C-terminal three TMS we first reinvestigated the topology of the C-terminal section of NCKX2. We substituted cysteine residues in locations that, in the 10 TMS model, are predicted

to be at extracellular C-terminus (S660), in the intracellular 9–10 loop (M628) and in the extracellular 8–9 loop (Q594), respectively; we also used the single endogenous cysteine residue located in the middle of the large cytosolic loop (C394) (Fig. 1, top panel). We expressed the cDNAs encoding these mutant NCKX2 proteins separately in High Five cells, then incubated the cells with 5 mM of the large (5 kDa) and hydrophilic MALPEG reagent and looked for “pegylated” mutant NCKX2 proteins by the expected increase in molecular weight. As shown before, the expressed NCKX2 protein invariably runs as a doublet representing full-length NCKX2 (upper band) and NCKX2 from which the N-terminal signal peptide is cleaved (lower band).⁴ In a first set of experiments we observed that the Q594C

and S660C mutant proteins invariably showed a band with an increased MW indicative of a “pegylated” fraction, whereas “pegylation” of the M628C and C394C mutant proteins was always less or almost nonexistent. To explore whether pegylation of the M628C and C394C mutant proteins reflected the presence of a fraction of leaky cells, we repeated this experiment but removed leaky cells by FACS prior to separation of cell proteins on SDS-PAGE and detection by western blotting. In four experiments representing separate transfections we observed the pegylation pattern illustrated in **Figure 2**: strong pegylation was observed for the Q594C and S660C mutant NCKX2 proteins whereas no pegylation was observed for the M628C and C394C mutant NCKX2 proteins. When the intracellular environment was made accessible to the hydrophilic MALPEG reagent after treatment with the permeabilizing reagent saponin, all four mutant NCKX2 proteins tested here showed a strong pegylated component consistent with the location of M628C and C394C in 9–10 linker and the cytosolic loop, resp. (**Fig. 2**). We also investigated many residues thought to be located near the middle of the membrane and did not observe any pegylation even in the presence of saponin; in such cases pegylation was only observed after the mutant protein was denatured by a strong detergent such as 1% SDS (data not illustrated). The pegylation results illustrated in **Figure 2** are consistent with the 10 TMS topological model of NCKX2 we reported before.⁹

Next, we selected three residues in the NCX1 protein that might help to distinguish between the two distinct topological models for NCX1 illustrated in **Figure 1** (bottom panel). In the current topological model of NCX1, the T907 residue of the NCX1 protein is thought to be located in the extracellular 8–9 linker and is expected to be accessible to MALPEG in the absence of any membrane permeabilizing agent like saponin. Conversely, the G870C and F938C residues are expected to become accessible to MALPEG only in the presence of saponin. In contrast, the 10 TMS topological model of NCX1 predicts the opposite result, i.e., pegylation of the G870C and F938C mutant NCX1 proteins in the absence of saponin. In four experiments we used FACS sorted cells and observed the pegylation pattern illustrated in **Figure 3**. The G870C and F938C mutant proteins could be pegylated in intact cells whereas the T907C mutant NCX1 protein was only pegylated in the presence of saponin. These results are very similar to those observed for NCKX2 and are consistent with the 10 TMS topological model of NCX1 (**Fig. 1**). Expression of the NCX1 and NCKX2 (mutant) proteins in High Five cells typically resulted in a significant fraction of the expressed protein located in internal membranes rather than the surface membrane (data not shown). Our mass-tagging assay

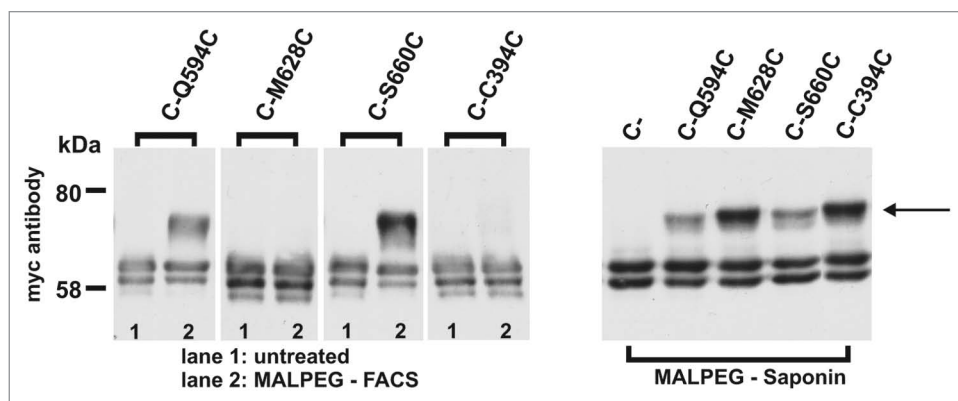


Figure 2. Mass-tagging of cysteine substitution mutants in the cysteine-free NCKX2 (C-). The indicated NCKX2 mutant proteins were expressed in High Five cells and subjected to mass-tagging with the 5 kDa MALPEG reagent as described under Materials and Methods. Shown are western blots for the myc-tagged NCKX2 protein obtained from cell extracts. Left panels show untreated cells (lane 1) and cells treated with MALPEG and then cell sorted with FACS (lane 2); right panel represent cells treated with MALPEG in the presence of saponin. The arrow indicates the pegylated protein. The observed mass shift always appeared greater than 5 kDa, presumably due to the distinct physicochemical nature of PEG.

selects for protein correctly trafficked to the surface membrane and this is most likely the reason for the incomplete pegylation observed in all our experiments. Complete pegylation was only observed after cell membranes were fully dissolved in strong denaturing detergents such as 1% SDS (data not shown). Trafficking to the surface membrane suggests that the mutant NCX1 and NCKX2 proteins were correctly folded and reflects the topology of the WT NCX1 and NCKX2 proteins, respectively. To further investigate whether the various mutant NCX1 and NCKX2 proteins used in this study yield functional $\text{Na}^+/\text{Ca}^{2+}$ exchangers we performed ^{45}Ca uptake experiments as described previously;¹⁹ in these experiments we measured ^{45}Ca uptake in Na^+ -loaded cells which represents so-called reverse $\text{Na}^+/\text{Ca}^{2+}$ exchange (**Fig. 4**). As shown in **Figure 4** all the mutant NCX1 and NCKX2 proteins showed significant $\text{Na}^+/\text{Ca}^{2+}$ exchange activity and represented functionally active exchanger proteins. The transport activities of the cysteine-free NCX1 and NCKX2 were about 50% of those observed for WT NCX1 and NCKX2, respectively. It should be pointed out that the cysteine-free NCX1 showed poor function when expressed in High Five cells unless the cell membranes were supplemented with cholesterol as described under Materials and Methods; this is the protocol used for the NCX1 experiments shown in **Figure 4**. Supplementation with cholesterol did not affect the pegylation experiments.

Insertion of N-glycosylation sites in bovine heart NCX1. In our earlier study on the topology of the NCKX2 protein we used insertion of *N*-glycosylation sites in all the loops linking the various TMS to assess their orientation (the single endogenous *N*-glycosylation site was removed).⁹ Here, we used the same strategy for the C-terminus and the preceding connecting loop of bovine NCX1 from which the single endogenous *N*-glycosylation site at the N-terminus was removed. We inserted the same spacer (SHV DHI SAE TEM EGE GNE TGE CTG SY Y CKK GVI LPI WED EP) containing a single *N*-glycosylation site in two separate constructs, one between residues G900 and E901

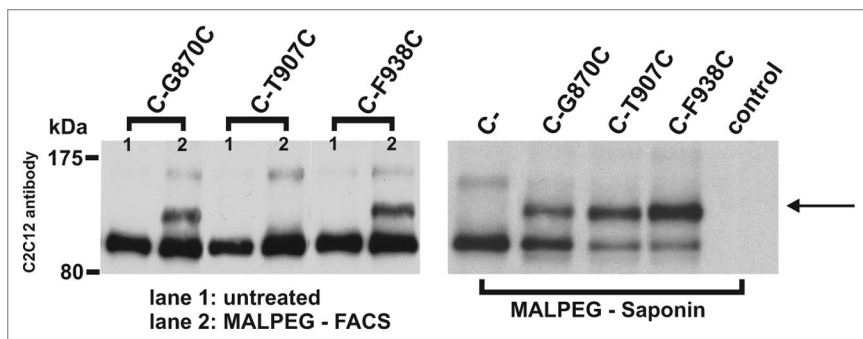


Figure 3. Mass-tagging of cysteine substitution mutants in the cysteine-free NCX1 (C-). The indicated mutant NCX1 proteins were expressed in High Five cells and subjected to mass-tagging with the 5 kDa MALPEG reagent as described under *Materials and Methods*. Shown are Western blots for the dNCX1 protein (C2C12 antibody) obtained from cell extracts. Left panels show untreated cells (lane 1) and cells treated with MALPEG and then sorted with FACS (lane 2); right panel represent cells treated with MALPEG in the presence of saponin. The arrow indicates the pegylated protein. As seen with mass-tagging of NCKX2, the observed mass shift always appeared greater than 5 kDa, presumably due to the distinct physicochemical nature of PEG.

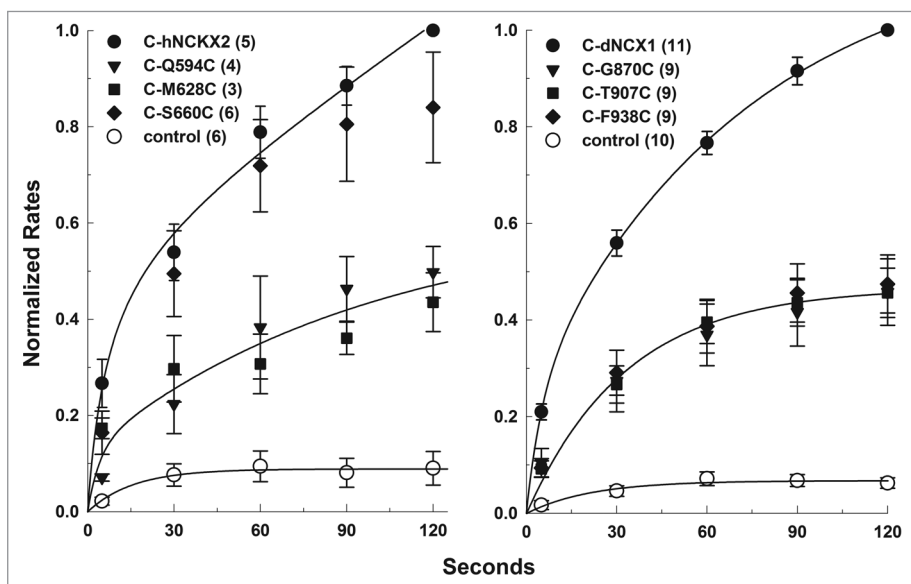


Figure 4. Functional activity of the mutant NCX1 and NCKX2 proteins expressed in High Five cells. High Five cells were transiently transfected with the indicated NCX1 and NCKX2 mutant cDNAs and transport function was measured two days post transfection. High Five cells were Na^+ -loaded with the use of the ionophore monensin and ^{45}Ca uptake was measured using a filtration assay as described previously.¹⁹ NCX or NCKX activity is defined as the difference in time-dependent ^{45}Ca uptake measured in 150 mM KCl medium and that measured in 150 mM NaCl medium. In addition to NaCl or KCl, the uptake medium contained 80 mM sucrose, 20 mM Hepes (adjusted to pH 7.4 with arginine), 10 μM EDTA and 1 μM FCCP. ^{45}Ca uptake was initiated at time zero by the addition of 1 μCi ^{45}Ca and 30 μM CaCl_2 and measured at 25°C. Open circles represent High Five cells transfected with empty vector. Left panel (NCKX2 mutants): filled circles, cysteine-free NCKX2 (C-); inverted triangles, C-Q594C; squares, C-M628C; diamonds, C-S660C. Right panel (NCX1 mutants): filled circles, cysteine-free NCX1 (C-); inverted triangles, C-G870C; squares, C-T907C; diamonds, C-F938C. Data are normalized to uptake seen in cells expressing the respective cysteine-free NCX1 and NCKX2 proteins; shown are average \pm standard error of the mean of 3 to 11 separate experiments.

(located in the 9–10 linker) and the other between H934 and I935 (at the C-terminus; the C-termini are highly conserved between dog and bovine NCX1 and have the same residue numbers). As illustrated in Figure 5, PNGase treatment of the C-terminus insert resulted in a slight lowering of the MW suggesting the spacer inserted at the C-terminus was glycosylated, hence, exposed to the extracellular space. No molecular weight shift was noticed for the 9–10 linker insert suggesting that this insert is exposed to the intracellular space. When we examined NCX function by means of ^{45}Ca uptake, the NCX1 mutant construct with the glycosylation site inserted at the C-terminus showed ^{45}Ca transport activity but the construct with the glycosylation site inserted into the 9–10 linker did not. These results are consistent with the pegylation experiments and with a 10 TMS topology for NCX1.

Discussion

In this study we reassessed the reported topological models of the mammalian NCX1^{6,7} and NCKX2⁹ $\text{Na}^+/\text{Ca}^{2+}$ ($-\text{K}^+$) exchangers motivated by the recently published crystal structure of a archaeobacterial $\text{Na}^+/\text{Ca}^{2+}$ exchanger.¹⁰ As the major difference in the reported topologies is centered on the C-terminal three TMS (Fig. 1) we focused on this region. We selected mass-tagging with the large (5 kDa) and hydrophilic MALPEG reagent in order to minimize access of the reagent to aqueous ion transport pathways within the NC(K)X protein that might allow penetration of smaller reagents, and, moreover, this reagent selects for detection of NC(K)X protein that is trafficked to the plasma membrane and is likely to represent the correctly folded NC(K)X protein. The mass-tagging experiments illustrated in Figures 2 and 3 are consistent with the 10 TMS topological model for both NCX1 and NCKX2. In the final stages of writing this manuscript we learned of a very recent study by Ren and Philipson²⁰ presenting cross-linking data that also support the 10TMS topology for NCX1. Combined with our data presented here this suggests strongly that the mammalian NCX and NCKX share the same 10 TMS topology with the archaeobacterial NCX_Mj. This

information should be useful in the interpretation of structure/function studies and assist homology modeling of mammalian NC(K)X based on the NCX_Mj structure.

Materials and Methods

General methods and materials. Cell culture (we used a lepidopteron insect cell expression system, BTI-TN-5B1-4 High Five™ cells, Invitrogen), transfection protocols, SDS-PAGE, ⁴⁵Ca uptake protocols and mutagenesis were all performed as described in detail before.^{14,19} All chemicals were purchased from Sigma unless stated otherwise. Single cysteine substitutions were made in the cysteine-free and myc-tagged human NCKX2 as described before.¹⁸ The cysteine-free dog NCX1 cDNA, cDNAs encoding single cysteine substitutions in it, and the R3F1 antibody were gifts from Drs D.A. Nicoll and K.D. Philipson. Bovine NCX1 cDNA was a gift of Dr J.P. Reeves.

MALPEG treatment and FACS analysis.

Methoxy-polyethylene glycol maleimide (MALPEG, JenKem Technology, A3125-1) treatment was performed on transiently transfected High Five cells expressing the indicated NCX1 or NCKX2 mutant proteins. Two days post transfection, cells were washed twice with sodium-Hepes buffer (150 mM NaCl, 80 mM Sucrose, 1 mM DTT, 20 mM Hepes, pH 7.4). The cells were resuspended in the sodium-Hepes buffer (with 0.1 mM DTT) to which was added a final concentration of 5 mM freshly dissolved MALPEG. For samples treated with saponin and MALPEG, 0.02% (final concentration) saponin was added to the 5 mM MALPEG solution. The cells were then incubated for 15 min at room temperature with gentle mixing. The reaction was terminated by the addition of 5 mM reduced glutathione and 1 mM EDTA. After this, the cells were spun down (3,000 g, 3 min) and washed twice with the sodium-Hepes buffer containing 0.1 mM N-ethyl maleimide to modify all remaining free thiol groups. The samples were then taken for fluorescence activated cell sorting (FACS) at the Flow Cytometry Facility at the University of Calgary. We removed leaky cells by FACS using propidium iodide.²¹

Cholesterol supplementation of High Five cells. High Five cells were supplemented with cholesterol using a methyl-β-cyclodextrin vehicle. Preparation of the cholesterol-methyl-β-cyclodextrin complex was performed in the following manner. One g of methyl-β-cyclodextrin was dissolved at 80°C in 5 ml of double distilled water. Thirty mg of cholesterol was dissolved in 1 ml of ethanol and added to the methyl-β-cyclodextrin solution which was stirred until clear. The combined solution was distributed into microvials, freeze-dried for a 24 h period

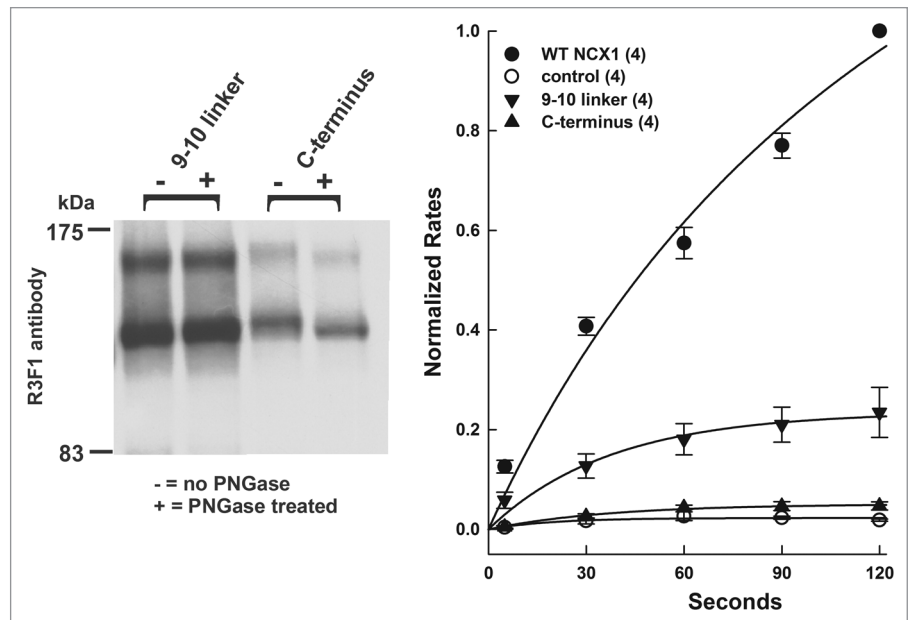


Figure 5. Insertion of *N*-glycosylation sites at two separate positions in the C-terminal section of bovine NCX1. Left panel: The indicated mutant NCX1 proteins were expressed in High Five cells and subjected to PNGase treatment as described under *Materials and Methods*. Shown are western blots for the bNCX1 protein (R3F1 antibody) obtained from cell extracts (very similar results were obtained in four other experiments). *N*-glycosylation sites were introduced in the 9–10 linker or at the C-terminus as described in the text. Right panel: Exchange function was assessed by ⁴⁵Ca uptake as described in detail in the legend of **Figure 4**. Data are normalized to uptake seen in the WT bNCX1 and represent average ± standard error of the mean of 4 separate experiments.

and then stored at room temperature. Immediately prior to cell treatment with the cyclodextrin-cholesterol complex, double distilled water was added to make a 10 mM cholesterol-methyl-β-cyclodextrin solution. The High Five Cell media was replaced 24 h post transfection with 3 ml of complete HyQ-IPL-41 media supplemented with 0.15 mM cholesterol-methyl-β-cyclodextrin. The cells were then incubated for another 24 h at 28°C, at which time they were collected and washed two times in sodium-HEPES buffer.

Glycosidase treatment. Transiently transfected High Five cells were collected two days post transfection and washed two times in sodium-Hepes buffer. The cell pellets were resuspended in a small volume of ice cold RIPA lysis buffer made up of 140 mM NaCl, 25 mM Tris, 1% Triton X-100, 0.5% sodium deoxycholate, 0.1 mM EDTA, pH 7.5, and protease inhibitors (Roche Diagnostics, 05892791001). Following 20 min of incubation on ice, RIPA extracts were spun down at 20,000 g for 5 min at 4°C and the supernatants were collected. The protein content of the supernatants was determined with the Bio-Rad protein assay (Bio-Rad Laboratories, 500-0006). Protein samples were denatured by incubating them in 1% β-mercaptoethanol and 0.5% SDS for 10 min at 37°C. Following this incubation, 1% NP-40 and 50 mM Na₂PO₄ were added to neutralize the denaturing conditions. The glycosidase PNGase F (New England Biolabs P0704S) was then added to the samples to a final concentration of 2 units/μl. The samples were incubated for 1.5 h in a 37°C

water bath. Sample buffer (62.5 mM TRIS-HCl, pH 6.8, 2% (w/v) SDS, 10% glycerol, 41 mM DTT, and 0.03% (w/v) phenol red) was added and the samples were analyzed by SDS-PAGE and western blotting.

Western blotting. The Following monoclonal antibodies were used: Myc-Tag (9B11) mouse mAB (New England Biolabs, 2276), anti-NCX1 C2C12 mouse mAB (Affinity Bioreagents MA3926) and anti-NCX1 R3F1 mouse mAB in TBST (10 mM Tris, 100 mM NaCl, 0.05% Tween 20, pH 8.0 with HCl) supplemented with 1% skim milk. The nitrocellulose membranes were blocked for 1 h with TBST-5% skim milk, then incubated overnight at a 1:1,000 dilution of primary antibody in TBST-1% skim milk and then washed four times with 20 ml of TBST. Next, the membranes were incubated in the dark with a 1:20,000 dilution of Goat anti-mouse IRDye 800CW

(Mandel Scientific, 926-32210) in TBST-1% skim milk for 1 h at room temperature. The membranes were washed four times with TBST, rinsed with 10 ml of de-ionized water and scanned on the LI-COR Odyssey Infrared Imager.

Disclosure of Potential Conflicts of Interest

No potential conflicts of interest were disclosed.

Acknowledgments

We thank Drs K.D. Philipson and D.A. Nicol for reagents (dNCX1 cDNAs, R3F1 antibody) and sharing the protocol for cholesterol supplementation of High Five cells, and Dr J.P. Reeves for the bNCX1 cDNA. This work was supported through operating grant MOP-81327 from the Canadian Institutes for Health Research.

References

1. Altimimi HF, Schnetkamp PPM. Na⁺/Ca²⁺-K⁺ exchangers (NCKX): functional properties and physiological roles. *Channels (Austin)* 2007; 1:62-9; PMID:18690016.
2. Lytton J. Na⁺/Ca²⁺ exchangers: three mammalian gene families control Ca²⁺ transport. *Biochem J* 2007; 406:365-82; PMID:17716241; <http://dx.doi.org/10.1042/BJ20070619>.
3. Schnetkamp PPM. The *SLC24* gene family of Na⁺/Ca²⁺-K⁺ exchangers: from sight and smell to memory consolidation and skin pigmentation. *Mol Aspects Med* 2013; 34:455-64; <http://dx.doi.org/10.1016/j.mam.2012.07.008>
4. Kang KJ, Schnetkamp PPM. Signal sequence cleavage and plasma membrane targeting of the retinal rod NCKX1 and cone NCKX2 Na⁺/Ca²⁺ - K⁺ exchangers. *Biochemistry* 2003; 42:9438-45; PMID:12899631; <http://dx.doi.org/10.1021/bi0342261>.
5. Sahin-Tóth M, Nicoll DA, Frank JS, Philipson KD, Friedlander M. The cleaved N-terminal signal sequence of the cardiac Na⁺-Ca²⁺ exchanger is not required for functional membrane integration. *Biochem Biophys Res Commun* 1995; 212:968-74; PMID:7626138; <http://dx.doi.org/10.1006/bbrc.1995.2064>.
6. Nicoll DA, Ottolia M, Lu L, Lu Y, Philipson KD. A new topological model of the cardiac sarcolemmal Na⁺-Ca²⁺ exchanger. *J Biol Chem* 1999; 274:910-7; PMID:9873031; <http://dx.doi.org/10.1074/jbc.274.2.910>.
7. Iwamoto T, Nakamura TY, Pan Y, Uehara A, Imanaga I, Shigekawa M. Unique topology of the internal repeats in the cardiac Na⁺/Ca²⁺ exchanger. *FEBS Lett* 1999; 446:264-8; PMID:10100855; [http://dx.doi.org/10.1016/S0014-5793\(99\)00218-5](http://dx.doi.org/10.1016/S0014-5793(99)00218-5).
8. Cai X, Zhang K, Lytton J. A novel topology and redox regulation of the rat brain K⁺-dependent Na⁺/Ca²⁺ exchanger, NCKX2. *J Biol Chem* 2002; 277:48923-30; PMID:12377762; <http://dx.doi.org/10.1074/jbc.M208818200>.
9. Kinjo TG, Szerencsei RT, Winkfein RJ, Kang KJ, Schnetkamp PPM. Topology of the retinal cone NCKX2 Na⁺/Ca-K exchanger. *Biochemistry* 2003; 42:2485-91; PMID:12600216; <http://dx.doi.org/10.1021/bi0270788>.
10. Liao J, Li H, Zeng W, Sauer DB, Belmares R, Jiang Y. Structural insight into the ion-exchange mechanism of the sodium/calcium exchanger. *Science* 2012; 335:686-90; PMID:22323814; <http://dx.doi.org/10.1126/science.1215759>.
11. Nicoll DA, Hryshko LV, Matsuoka S, Frank JS, Philipson KD. Mutation of amino acid residues in the putative transmembrane segments of the cardiac sarcolemmal Na⁺-Ca²⁺ exchanger. *J Biol Chem* 1996; 271:13385-91; PMID:8662775; <http://dx.doi.org/10.1074/jbc.271.23.13385>.
12. Ottolia M, Nicoll DA, Philipson KD. Mutational analysis of the alpha-1 repeat of the cardiac Na⁺-Ca²⁺ exchanger. *J Biol Chem* 2005; 280:1061-9; PMID:15519995; <http://dx.doi.org/10.1074/jbc.M411899200>.
13. Altimimi HF, Fung EH, Winkfein RJ, Schnetkamp PP. Residues contributing to the Na⁺-binding pocket of the SLC24 Na⁺/Ca²⁺-K⁺ Exchanger NCKX2. *J Biol Chem* 2010; 285:15245-55; PMID:20231282; <http://dx.doi.org/10.1074/jbc.M109.090738>.
14. Winkfein RJ, Szerencsei RT, Kinjo TG, Kang KJ, Perizzolo M, Eisner L, et al. Scanning mutagenesis of the alpha repeats and of the transmembrane acidic residues of the human retinal cone Na⁺/Ca-K exchanger. *Biochemistry* 2003; 42:543-52; PMID:12525183; <http://dx.doi.org/10.1021/bi026982x>.
15. Kang KJ, Kinjo TG, Szerencsei RT, Schnetkamp PPM. Residues contributing to the Ca²⁺ and K⁺ binding pocket of the NCKX2 Na⁺/Ca²⁺-K⁺ exchanger. *J Biol Chem* 2005; 280:6823-33; PMID:15583008; <http://dx.doi.org/10.1074/jbc.M407933200>.
16. Kang KJ, Shibukawa Y, Szerencsei RT, Schnetkamp PPM. Substitution of a single residue, Asp⁵⁷⁵, renders the NCKX2 K⁺-dependent Na⁺/Ca²⁺ exchanger independent of K⁺. *J Biol Chem* 2005; 280:6834-9; PMID:15611132; <http://dx.doi.org/10.1074/jbc.M412933200>.
17. Lu J, Deutsch C. Pegylation: a method for assessing topological accessibilities in Kv1.3. *Biochemistry* 2001; 40:13288-301; PMID:11683639; <http://dx.doi.org/10.1021/bi0107647>.
18. Kinjo TG, Szerencsei RT, Winkfein RJ, Schnetkamp PPM. Role of cysteine residues in the NCKX2 Na⁺/Ca²⁺-K⁺ Exchanger: generation of a functional cysteine-free exchanger. *Biochemistry* 2004; 43:7940-7; PMID:15196038; <http://dx.doi.org/10.1021/bi049538y>.
19. Prinsen CFM, Szerencsei RT, Schnetkamp PPM. Molecular cloning and functional expression of the potassium-dependent sodium-calcium exchanger from human and chicken retinal cone photoreceptors. *J Neurosci* 2000; 20:1424-34; PMID:10662833.
20. Ren X, Philipson KD. The topology of the cardiac Na⁺/Ca²⁺ exchanger, NCX1. *J Mol Cell Cardiol* 2013; 57C:68-71; PMID:23376057; <http://dx.doi.org/10.1016/j.yjmcc.2013.01.010>.
21. Sasaki DT, Dumas SE, Engleman EG. Discrimination of viable and non-viable cells using propidium iodide in two color immunofluorescence. *Cytometry* 1987; 8:413-20; PMID:3113897; <http://dx.doi.org/10.1002/cyto.990080411>.
22. Schwarz EM, Benzer S. Calx, a Na-Ca exchanger gene of *Drosophila melanogaster*. *Proc Natl Acad Sci U S A* 1997; 94:10249-54; PMID:9294196; <http://dx.doi.org/10.1073/pnas.94.19.10249>.